Modeling Hydrocarbons Adsorption in Amorphous Nanoporous Carbonaceous Materials

Nicholas J. Corrente¹, Elizabeth L. Hinks¹, Aastha Kasera¹, Raleigh Gough¹, Peter I. Ravikovitch², and Alexander V. Neimark^{1*}

¹Department of Chemical and Biochemical Engineering, Rutgers, The State University of New Jersey, Piscataway, New Jersey 08854, United States

²Corporate Strategic Research, ExxonMobil Research and Engineering Company, Annandale, New Jersey 08801, United States

*Corresponding author. Tel: 848-445-0834 Email: aneimark@rutgers.edu
Keywords: Gas adsorption, pore size characterization, nanoporous materials, carbons, hydrocarbons

Abstract

Predicting adsorption on nanoporous carbonaceous materials is important for developing various adsorption and membrane separations, as well as for oil and gas recovery from shale reservoirs. Here, we explore the capabilities of 3D molecular models of disordered carbon structures to reproduce the morphological and adsorption features of practical adsorbents. Using grand canonical Monte Carlo simulations, we construct a series of adsorption isotherms of simple fluids (N₂, Ar, CO₂, and SO₂) and a series of alkanes from methane to hexane on two model 3D structures, purely microporous structure A and micro-mesoporous structure B. We show that structure A reproduces the morphological properties of commercial Norit R1 Extra activated carbon and demonstrates outstanding agreement between the simulated and experimental adsorption isotherms reported in the literature for all adsorbates considered. Good agreement is also found for simulated and measured isosteric heats. Taking into account inherent variability of structural properties of commercial carbons and experimental adsorption data from different literature sources, the correlations with experiments are truly amazing. This work provides a new insight into the specifics of structural and adsorption properties of nanoporous carbons and demonstrates the advantages of using 3D molecular models for predicting adsorption hydrocarbons and other chemicals by MC simulations.

1 Introduction

Nanoporous carbons, such as activated carbons, carbon fibers, and carbon molecular sieves, have many practical industrial applications for mixture separations, [1] hydrocarbon storage, [2] and electrodes. [3] Unlike crystalline solids of regular and well-characterized structure, nanoporous carbons are composed of arrangements of disordered graphitic domains. This amorphous configuration provides for highly tortuous internal surfaces and pores of various shapes and sizes forming a disordered 3-dimensional pore network. It is of paramount importance to create realistic structural models, which can be used for pore structure characterization and capable of predicting adsorption of various gases and their mixtures in the wide range of pressures and temperatures. Conventional methods of pore structure characterization rely on oversimplified slit-shaped and cylindrical pore models, which do not capture the nanoscale specifics of carbon disordered structures. [4-13]

Considerable effort has been devoted to developing theoretical and computational methods for generating molecular models of amorphous carbons. ^[14] The Hybrid Reverse Monte Carlo (HRMC) method uses MC simulations to reproduce the experimental radial distribution functions (RDF). ^[15-20] HRMC method was employed by Opletal et al. ^[21] to construct 3D models of silicon and carbon structures. Kowalczyk et al ^[22] generated atomic structures of nanopore surfaces in oxidized and non-oxidized activated carbon fibers using temperature quench MC simulations (TQ-MC) with the bond-making bond-breaking reactive environment-dependent interaction potential carbon potential (EDIP). The authors applied this model to analyze the formaldehyde adsorption affected by co-adsorption of water.

Another group of methods are based on Molecular Dynamics (MD) simulations to generate carbon structures. ^[23-25] The Quench Molecular Dynamics (QMD) methods were used by Palmer et al. ^[26] to construct amorphous carbon models starting from high-temperature liquid carbon. The authors showed that increasing degrees of ordering can be achieved by slowing the quench rate. Wang et al. ^[27]

employed machine learning (ML) techniques to calculate the intermolecular potentials for carbon structures. The authors utilized an ML-based Gaussian approximation potential, which fits interatomic potentials to quantum-mechanical calculations performed on graphite and activated carbons, to generate 3D structures from a high-temperature liquid carbon precursor. The structures were graphitized at high temperatures and then annealed at room temperature using MD simulations.

DeTomas et al. ^[28, 29] employed annealing, rather than quenching, to generate amorphous carbon structures. The Annealed MD (AMD) was combined with the EDIP forcefield ^[30] which was parameterized for carbon structures by Marks. ^[31] This extended EDIP forcefield has the advantage of a longer cutoff (0.32 nm), which allows for increased layering of defective graphene sheets. The authors built the 3D structures that exhibit the graphitization that is lacking in QMD-generated structures. The ordering and graphitization of the structures was correlated with the increase in annealing temperature. These models, some of which are considered in this work, are included in the Database of Porous Rigid Amorphous Materials. ^[32]

The goal of this work is to demonstrate the applicability of 3D molecular models in pore structure characterization and predicting adsorption of simple fluids and hydrocarbons on carbon materials. In Section 2, we present the methods employed for modeling 3D carbon structures selected in this work, the grand canonical Monte Carlo (GCMC) simulations of adsorption, and the geometric and adsorption pore structure characterization. In Section 3.1, we demonstrate the structural and adsorption properties on two selected 3D carbon structures, purely microporous structure A and micro-mesoporous structure B, by simulating adsorption isotherms of N₂ and Ar at normal boiling temperatures and CO₂ at 0 °C, the adsorbates that are commonly used for pore structure characterization. We discuss the specifics of adsorption on 3D carbon structures and compare the structural properties calculated using the simulated isotherms and obtained from the geometric methods. Section 3.2 presents the simulated adsorption isotherms of simple fluids (N₂, Ar, CO₂, SO₂) and a series of alkanes from methane to hexane

at room temperature. It is shown that the constructed isotherms on structure A agree well with the experimental isotherms on the Norit R1 Extra activated carbon. Perfect correlation is found also between the simulated and measured isosteric heats. Conclusions are summarized in Section 4.

2 Methods

2.1 Carbon Structures

Figure 1 shows the two 3D carbon models (aCarbon-Marks-id015 and aCarbon-Marks-id004) selected from the Database of Porous Rigid Amorphous Materials [32] denoted in this work as structure A (left) and structure B (right). The OVITO software was used to visualize the carbons. [33]

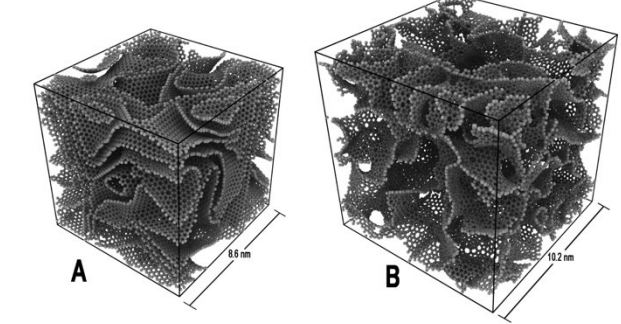


Figure 1: 3D carbon structures A (left) and B (right), ^[29] which were created using the AMD method described in Ref. ^[28]. The structures are composed of a comparable number of atoms in differently sized periodic boxes. Structure B is a more open structure, with a higher pore volume fraction of 0.65, which yields a broader pore size distribution than structure A.

Structures A and B were chosen for their distinct structural properties. Structure A was generated by annealing at 4000 K, and structure B was annealed at 2000 K; the higher annealing temperature allows for increased layer stacking and a greater degree of graphitization. ^[28] Both models A and B contain the same number (32,000) of carbon atoms in cubic periodic boxes of 8.6 nm and 10.2 nm, that correspond to the carbon densities of 1 g/cm³ and 0.6 g/cm³ and volume fractions of 0.49 and 0.7, respectively. The carbon models were shown to exhibit comparable Young's modulus values (20 GPa) to experimentally generated silicon carbide and titanium-derived 3D graphene networks. ^[32]

2.2 GCMC Simulations of Adsorption

GCMC simulations were employed to model adsorption of simple fluids (N₂, Ar, CO₂, SO₂) and hydrocarbons in selected 3D carbon structure models. The simulated adsorption isotherms were used to characterize the structures through the adsorption methods discussed in Sections 2.3 and 3.1, and to

compare with the experimental isotherms of fluids adsorbed in a commercially available activated carbon (see Section 3.2). The carbon atoms comprising the amorphous structures were modeled as Lennard-Jones (LI) spheres using parameters from Ref. [34]. Periodic boundary conditions were applied to the structures in all three dimensions. The argon adsorbate atoms were modeled as LI spheres using parameters from Ref. [35]. Nitrogen and carbon dioxide were modeled atomistically using the TraPPE force field, [36] and methane and alkanes were modeled with united-atom spheres using the TraPPE-UA forcefield. [37] Sulfur dioxide was simulated as a four-center model following Ref. [38]. Intermolecular interactions were simulated using Lorentz-Berthelot mixing rules. The parameters for each model are listed in the Supplementary Information, Section S3. GCMC simulations were performed using the RASPA open-source software package. [39] The systems were equilibrated for at least 25 million MC moves, and then a production run of at least 50 million MC moves was performed. For longer hydrocarbons, the number of equilibration and production moves was increased to 150 million MC moves to insure proper equilibration.

The isosteric heat of adsorption, $q_{\rm st}$, was computed in the course of GCMC simulations in the RASPA software from the fluctuations of the potential energy, U, and the number of adsorbed molecules, N, according to the following equation, [40]

$$q_{st} = RT - [\langle UN \rangle - \langle U \rangle \langle N \rangle] / [\langle N^2 \rangle - \langle N \rangle^2].$$

2.3 Characterization Methods

Geometric property calculations are performed using the PoreBlazer v4.0 open-source software. ^[41] The geometric method is based on probing the pore structure with virtual spherical particles of different radii and constructing the Connolly surface. ^[42] As related to adsorbent characterization, it was first used by Gelb and Gubbins with examples of 3D models of porous glasses. ^[43] The geometric surface and volume pore size distributions are associated with the areas and volumes enveloped by the Connolly surfaces. The diameter of the spherical probe of 0.3314 nm allows for a direct comparison with the

surface area and pore volume determined by the standard nitrogen adsorption characterization method. The geometric parameters reported in this work are calculated neglecting the effect of pore accessibility.

The standard methods of adsorption characterization are employed for calculating the pore volume, surface area, and PSD functions using the MC simulated isotherm as an input. The pore volume and specific surface area determined, respectively, by the Gurvich rule and the BET method modified by Rouquerol as recommended by IUPAC. [44] Calculations are performed with the NLDFT carbon slit pore model [45] implemented in the VersaWin software. [46]

3 Results and Discussion

3.1 Adsorption of Ar, N2, and CO2 and pore structure characterization of 3D carbon models.

We begin our studies of the 3D carbon models by simulating adsorption of nitrogen at 77.4 K, argon at 87.3 K, and carbon dioxide at 273 K from low pressures up to saturation, following the standard experimental conditions of most adsorption characterization measurements. Figure 2 A and B

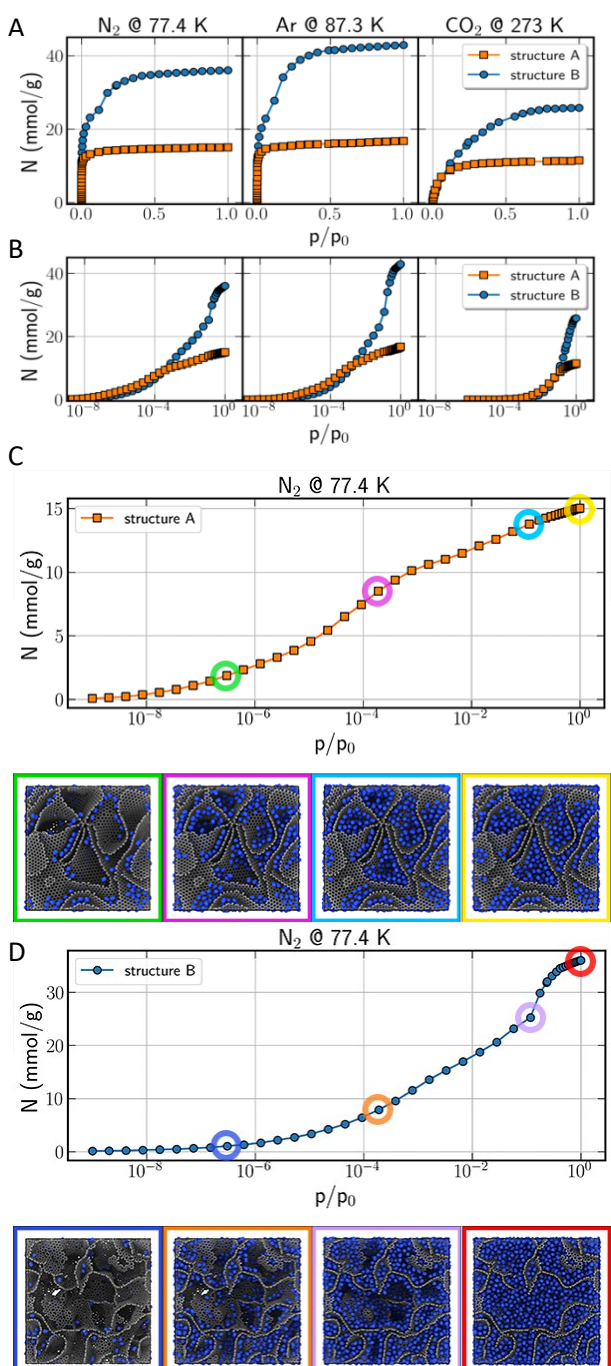


Figure 2: Adsorption isotherms of Nitrogen at 77.4 K (left), Argon at 87.3 K (center), and CO_2 at 273 K (right) in linear (A) and semi-log (B) scales up to saturation. Panels C and D show the individual N_2 isotherms with representative snapshots from the simulations.

show the isotherms obtained from GCMC simulations for structure A (orange squares) and structure B (blue circles). Panel A shows the adsorption in linear scale, panel B in semi-log scale. Adsorption isotherms on structure A are of the Type I isotherm according to IUPAC classifications, $^{[44]}$ typical for microporous materials. N_2 and Ar isotherms on structure B exhibit a more complex shape with pronounced adsorption at low pressures that is characteristic of micropores, and a step in uptake in the range of $p/p_0 \approx 0.1-0.2$, which indicates capillary condensation in small mesopores. Noteworthy, the isotherms on samples A and B almost coincide at low pressure ($p/p_0 < 10^{-4}$ for N_2 and Ar and $p/p_0 < 0.03$ for CO_2), as in this region adsorption is dominated by solid-fluid interactions with negligible confinement effects, and both models are composed of the same number of carbon atoms.

Figure 2, C and D show the calculated N_2 isotherms for structures A and B with the snapshots taken during the simulation. For both structures at low loadings, adsorption occurs on the carbon surfaces and in the smallest pores. The isotherm trend at low pressures is very similar in both structures despite the striking difference in pore morphology since the isotherms are presented on a per mass basis. As the pressure increases, the smallest pores are filled and layers begin forming on the walls of larger pores. The shape of the isotherm reflects the specifics of pore morphology. The isotherm on structure A saturates above $p/p_0 \approx 0.001$ that is characteristic for purely microporous systems. The isotherm on structure B gradually increases corresponding to monolayer formation at $p/p_0 \approx 0.1 - 0.2$ and further to capillary condensation at $p/p_0 \approx 0.2 - 0.3$ in mesopores of 2-3 nm in width. The process of adsorption and pore filling is illustrated by the snapshots of the adsorbate distributions in Figure 2 C and D. Note that the snapshots are taken for the same pressure points for both structures to demonstrate the similarity of adsorption mechanism at low pressures and its distinction at higher pressures. While pore filling of micropores in both structures proceeds without distinct formation of surface monolayers, monolayer build-up and consequent capillary condensation is pronounced in mesopores of structure B.

The simulated isotherms are employed to compare the extent to which the standard adsorption methods of pore structure characterization correlate with the geometric

Table 1: Surface areas and pore volumes calculated by geometric (PoreBlazer) and adsorption (BET and Gurvich) methods.

	Surface Area (m²/g)		Pore Volume (cm³/g)			
Structure	BET	Geometric	N ₂	Ar	CO ₂	Geometric
Structure A	1216	1055	0.52	0.48	0.56	0.49
Structure B	2463	2148	1.25	1.22	1.29	1.2

methods. Table 1 presents the surface areas and pore volumes calculated geometrically with PoreBlazer and with the BET method and Gurvich rule applied to the simulated isotherms. $^{[44]}$ The BET area exceeds the geometric area by \sim 15% for both structures. The Gurvich pore volumes calculated for different adsorbates using the respective bulk liquid densities are in reasonable agreement with the geometric pore volume that was determined with the probe diameter of the spherical model of N_2 . The pore volumes determined from CO_2 somewhat exceed those obtained from N_2 and Ar that is typical for microporous samples, as CO_2 is capable of penetrating into the narrowest ultra-micropores inaccessible for other adsorbates. The best agreement with the geometric and Gurvich volumes is found for Ar.

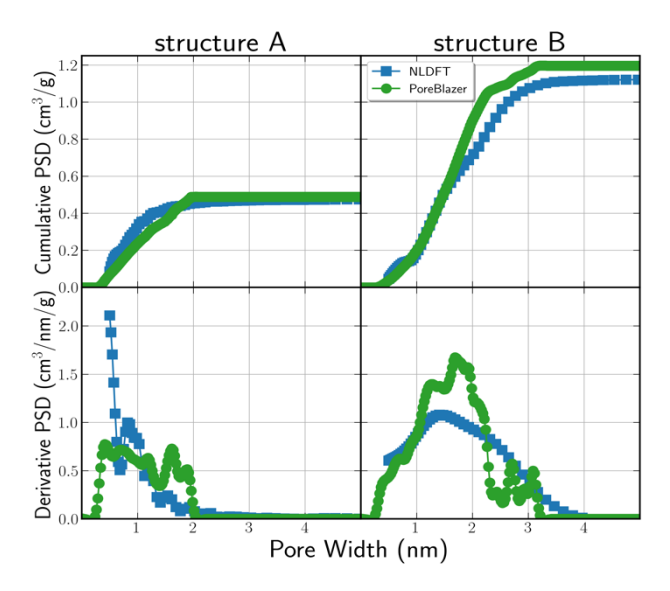


Figure 3: Pore size distributions for structure A (left) and structure B (right). Cumulative PSDs calculated with NLDFT kernels (blue squares) and PoreBlazer (green circles) are shown in the upper panels, and the corresponding derivative PSDs are shown on the bottom.

Figure 3 shows the cumulative (top) and derivative (bottom) PSDs calculated from the adsorption isotherms (blue) using the NLDFT method [45] and the geometric PoreBlazer method [41] (green) for structure A (left) and structure B (right). The PSDs quantify the polydispersity of pore channels. Structure B shows a broader PSD than structure A, with micropores (<2 nm) and narrow mesopores (2-4 nm). Structure A, that is denser with a lower porosity, is purely microporous. Agreement between the PSDs

obtained from adsorption and geometric methods is quite reasonable, despite that the NLDFT model is based on oversimplified representation of pores as slits between molecularly smooth walls.

3.2 Adsorption of simple fluids and hydrocarbons at room temperature. Correlation

with experiments.

The ultimate goal of developing structural models is their capability of predicting adsorption isotherms of chemicals of practical interest. To demonstrate the predictive capabilities of 3D carbon models, we constructed by GCMC simulations adsorption isotherms of N₂, CO₂, SO₂, and a series of alkanes from methane to hexane at room temperature of 298 K. In Figure 4, we present the results of simulations for structure A in comparison with the experimental data on Norit R1 Extra activated carbon acquired from different literature sources. [47-50] This carbon is a widely used adsorbent in various gas and liquid phase separations. [47-50] Although the pore volume of 0.626 cm³/g and BET surface area of 1430 m²/g reported for Norit R1

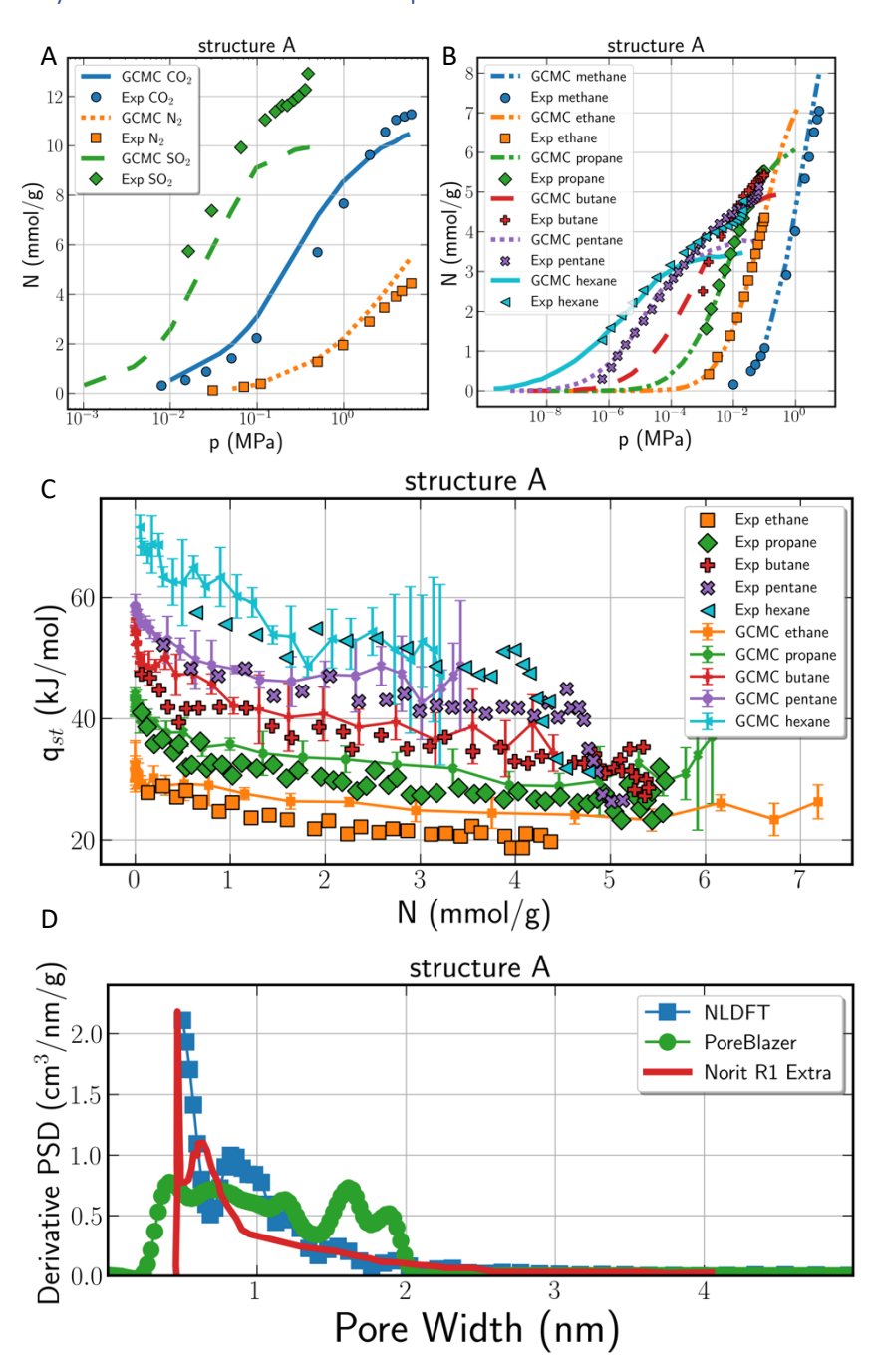


Figure 4: Correlation of GCMC adsorption isotherms of carbon dioxide, nitrogen, and sulfur dioxide (panel A) and hydrocarbons (panel B) at 298 K with experimental adsorption isotherms on Norit R1 Extra activated carbon from Refs. [47-50]. (C) The corresponding isosteric heats from alkane adsorption experiments and simulations. (D) Comparison of derivative PSDs from Figure 3 with the PSD for Norit R1 Extra [51] calculated using the Horvath-Kawazoe method. [52]

Extra [51] somewhat exceed the respective values for structure A (Table 1), there is a good qualitative agreement between the PSDs (Figure 4 D). Considering the inherent variability of structural parameters

of samples of commercial carbons employed by different groups, we may conclude that the structure A reproduces major morphological features of the Norit R1 Extra adsorbents.

Figure 4 A presents the adsorption of nitrogen (orange), carbon dioxide (blue), and sulfur dioxide (green) on structure A. The N₂ and CO₂ isotherms are in excellent agreement with experimental measurements. The simulated SO₂ isotherm has a similar qualitative shape yet somewhat underpredicts the adsorption isotherm, which is likely due to the homogeneous composition of the carbon structural model. The 3D structural models are composed entirely of non-polar carbon atoms, whereas the practical activated carbons contain both carbon atoms and polar functional groups, which may cause higher adsorption of polar adsorbates, such as sulfur dioxide.

Figure 4 B presents the simulated adsorption isotherms of hydrocarbons (lines) compared to the experimental adsorption isotherms (points) reported in Ref. [49]. The species simulated and their respective colors are noted in the figure legend. There is excellent agreement between the simulated and experimental isotherms for ethane and propane. However, for alkanes longer than propane, the computational model underpredicts adsorption at higher pressures. This is likely attributed to the difference in the structural properties of the computational and experimental structures: structure A has a pore volume of 0.49 cm³/g and a BET surface area of 1216 m²/g, whereas the Norit R1 Extra activated carbon has a pore volume of 0.626 cm³/g and a BET surface area of 1430 m²/g. [51] The larger pore volume and larger surface area of the experimental structure provides more space for the longer alkane molecules to adsorb.

Figure 4 C presents the isosteric heats of the chain hydrocarbons. The isosteric heat calculations exhibit significant fluctuations shown by error bars, there is good qualitative agreement. The magnitude of the isosteric heats and their trends are consistent between simulated and experimental results for all species. The isosteric heat monotonically decreases at low loadings, corresponding to the surface coverage of the pore walls, and achieve a plateau, corresponding to the pore filling. Also of note is the

slight increase and subsequent decrease of the isosteric heat for experimental hexane at high loadings.

This corresponds to the completion of the filling of the carbon, and subsequent capillary condensation in the binder used in the experimental setup. [49] This external space is not accounted for in the computational models.

The overall agreement of simulated and experimental data shown in Figure 4 is outstanding. It is worth noting that our GCMC simulations do not involve any adjustable parameters for the isotherm fitting. We use the standard molecular models recommended in the literature, as described above in

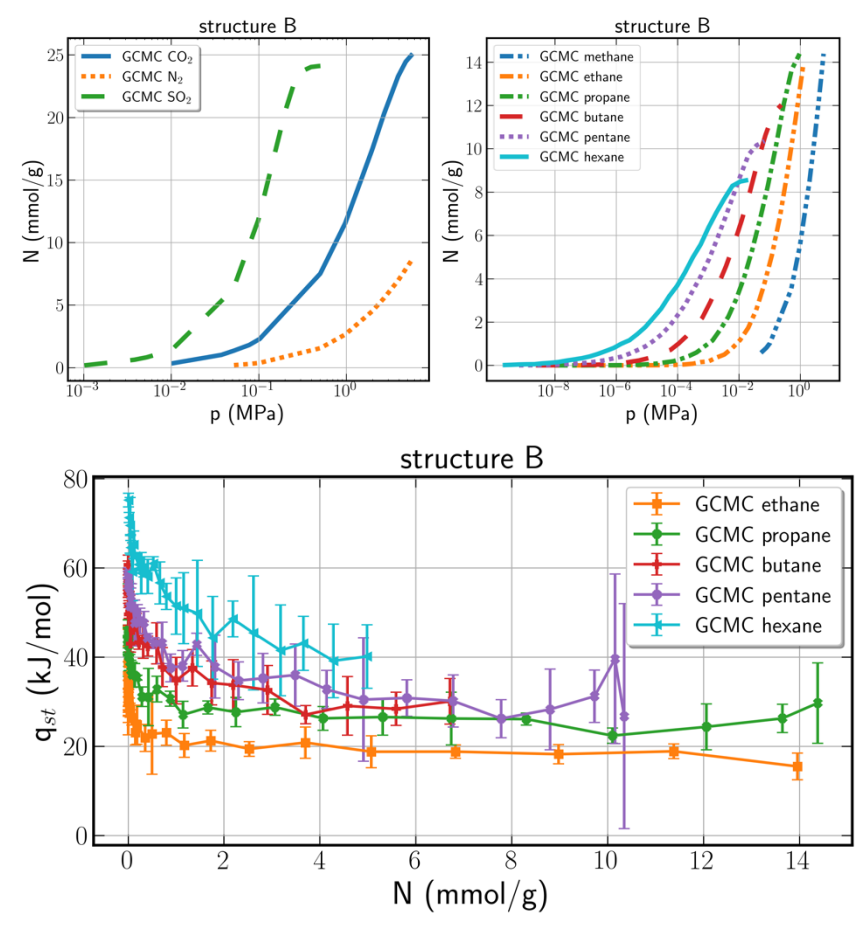


Figure 5: GCMC adsorption isotherms (top panels) and isosteric heats (bottom panel) for structure B simulated in the same systems as in Figure 4 for structure A.

Section 2.2.

In Figure 5 A, B, and C, we present the adsorption isotherms and isosteric heats simulated in structure B for the same adsorption systems as shown in Figure 4 for structure A. We do not have experimental data on carbons with comparable structural properties as structure B. Due to a larger porosity and broader pore size distribution that extends from micropores to mesopores, structure B shows a ~100% increase in adsorption

capacity over structure A for all adsorbates considered. The larger surface area and pore volume of structure B provides more room for each species to adsorb. This may suggest that carbons with a wide

PSD in the micropore and narrow (2-3 nm) mesopore ranges, may have advanced adsorption properties compared to purely microporous carbons like Norit 1 Extra.

4 Conclusions

We demonstrated the advantages and capabilities of using 3D molecular models for pore structure characterization and simulation of adsorption isotherms of various adsorbates on nanoporous carbons. These models exhibit disordered network of pores of different shapes and sizes between corrugated and defected fragments of graphene sheets. Two characteristic structural models developed by de Tomas et al. ^[29] were considered: purely microporous structure A and micro-mesoporous structure B. The model structures were characterized by geometric and adsorption methods. To this end, the isotherms of adsorption of N₂ at 77.4 K, Ar at 87.3 K, and CO₂ at 273 K were constructed by CGMC simulations. These simulations show the specifics of adsorption and pore filling in the interconnected micro- and mesopores. We found a reasonable agreement between the values of pore volume, specific surface area, and pore size distributions determined by the geometric PoreBlazer method and by the NLDFT methods from the simulated N₂ isotherms. We found that the pore structure properties of microporous structure A are similar to those of the commercial Norit R1 Extra activated carbon.

To compare with experimental data available in the literature, we simulated adsorption of N₂, CO₂, SO₂, and a series of alkanes from methane to hexane at room temperature of 298 K. We found excellent agreement between the simulated isotherms on structure A and experimental isotherms on Norit R1 Extra taken from different literature sources. Good correlations were also observed for the simulated and measured isosteric heats of ethane, propane, butane, pentane, and hexane. Taking into account that our GCMC simulations were based on the standard molecular models recommended in the literature and did not involve any adjustable parameters for the isotherm and isosteric heat fitting, the agreement with the experimental data is truly outstanding.

Structure A can be recommended as a benchmark for further investigations and extension of molecular simulation studies of other adsorption systems, including gas mixtures, that could be verified with experiments on Norit R1 Extra. 3D molecular models, exemplified here with structures A and B, can be employed for screening of optimal structural properties of nanoporous carbons with advanced adsorption properties for specific applications. Simulations with structure B, which in addition to micropores possess narrow (2-3 nm) mesopores, showed increased adsorption capacity compared to purely microporous structure A. Further work can be done with molecular models of various morphological types available in materials structures databases. These structures can be modified by incorporating various functional groups, ions, and ligands on carbon surfaces. The use of 3D molecular models opens up appealing opportunities for analyses off morphological and adsorption properties of existing materials and for computational screening and informed design of novel carbonaceous adsorbents with improved characteristics.

References

- 1. Peng, X.; Vicent-Luna, J. M.; Jin, Q., Separation of CF4/N2, C2F6/N2, and SF6/N2 Mixtures in Amorphous Activated Carbons Using Molecular Simulations. *ACS applied materials & interfaces* **2020**, *12* (17), 20044-20055.
- 2. El-Sharkawy, I. I.; Mansour, M. H.; Awad, M. M.; El-Ashry, R., Investigation of natural gas storage through activated carbon. *Journal of Chemical & Engineering Data* **2015**, *60* (11), 3215-3223.
- 3. Merlet, C.; Rotenberg, B.; Madden, P. A.; Taberna, P.-L.; Simon, P.; Gogotsi, Y.; Salanne, M., On the molecular origin of supercapacitance in nanoporous carbon electrodes. *Nature materials* **2012**, *11* (4), 306-310.
- 4. Yang, K.; Lu, X.; Lin, Y.; Neimark, A. V., Deformation of coal induced by methane adsorption at geological conditions. *Energy Fuels* **2010**, *24* (11), 5955-5964.
- 5. Yang, K.; Lu, X.; Lin, Y.; Neimark, A. V., Effects of CO2 adsorption on coal deformation during geological sequestration. *J. Geophys. Res. Solid Earth* **2011**, *116* (B8).
- 6. Corrente, N. J.; Dobrzanski, C. D.; Gor, G. Y., Compressibility of supercritical methane in nanopores: A molecular simulation study. *Energy Fuels* **2020**, *34* (2), 1506-1513.
- 7. Liu, J.; Wang, L.; Xi, S.; Asthagiri, D.; Chapman, W. G., Adsorption and phase behavior of pure/mixed alkanes in nanoslit graphite pores: an iSAFT application. *Langmuir* **2017**, *33* (42), 11189-11202.
- 8. Liu, J.; Xi, S.; Chapman, W. G., Competitive sorption of CO2 with gas mixtures in nanoporous shale for enhanced gas recovery from density functional theory. *Langmuir* **2019**, *35* (24), 8144-8158.
- 9. Gauden, P. A.; Terzyk, A. P.; Furmaniak, S.; Kowalczyk, P., Adsorption potential distributions for carbons having defined pore structure—GCMC simulations of the effect of heterogeneity. *Adsorption* **2009**, *15* (2), 99-113.
- 10. Lithoxoos, G. P.; Peristeras, L. D.; Boulougouris, G. C.; Economou, I. G., Monte Carlo simulation of carbon monoxide, carbon dioxide and methane adsorption on activated carbon. *Mol. Phys.* **2012**, *110* (11-12), 1153-1160.
- 11. Chen, G.; An, Y.; Shen, Y.; Wang, Y.; Tang, Z.; Lu, B.; Zhang, D., Effect of pore size on CH4/N2 separation using activated carbon. *Chin. J. Chem. Eng.* **2020**, *28* (4), 1062-1068.
- 12. Hermosilla, M.; Albesa, A., Monte Carlo simulations of simple gases adsorbed onto graphite and molecular models of activated carbon. *Adsorption* **2020**, *26* (8), 1301-1322.
- 13. Rouquerol, J.; Rouquerol, F.; Llewellyn, P.; Maurin, G.; Sing, K. S., *Adsorption by powders and porous solids: principles, methodology and applications*. Academic press: 2013.
- 14. Bhatia, S. K., Characterizing structural complexity in disordered carbons: from the slit pore to atomistic models. *Langmuir* **2017**, *33* (4), 831-847.
- 15. Kowalczyk, P.; Gauden, P. A.; Furmaniak, S.; Terzyk, A. P.; Wiśniewski, M.; Ilnicka, A.; Łukaszewicz, J.; Burian, A.; Włoch, J.; Neimark, A. V., Morphologically disordered pore model for characterization of micro-mesoporous carbons. *Carbon* **2017**, *111*, 358-370.
- 16. Kowalczyk, P.; Terzyk, A. P.; Gauden, P. A.; Furmaniak, S.; Wiśniewski, M.; Burian, A.; Hawelek, L.; Kaneko, K.; Neimark, A. V., Carbon molecular sieves: reconstruction of atomistic structural models with experimental constraints. *J. Phys. Chem. C* **2014**, *118* (24), 12996-13007.
- 17. Ishida, M.; Ohba, T., Hybrid reverse molecular dynamics simulation as new approach to determination of carbon nanostructure of carbon blacks. *Scientific reports* **2020**, *10* (1), 1-8.
- 18. Jain, S. K.; Pellenq, R. J.-M.; Pikunic, J. P.; Gubbins, K. E., Molecular modeling of porous carbons using the hybrid reverse Monte Carlo method. *Langmuir* **2006**, *22* (24), 9942-9948.

- 19. Nguyen, T. X.; Cohaut, N.; Bae, J.-S.; Bhatia, S. K., New method for atomistic modeling of the microstructure of activated carbons using hybrid reverse Monte Carlo simulation. *Langmuir* **2008**, *24* (15), 7912-7922.
- 20. Farmahini, A. H.; Bhatia, S. K., Hybrid Reverse Monte Carlo simulation of amorphous carbon: Distinguishing between competing structures obtained using different modeling protocols. *Carbon* **2015**, *83*, 53-70.
- 21. Opletal, G.; Petersen, T. C.; O'Malley, B.; Snook, I.; McCulloch, D.; Yarovsky, I., HRMC: Hybrid Reverse Monte Carlo method with silicon and carbon potentials. *Comput. Phys. Commun.* **2008**, *178* (10), 777-787.
- 22. Kowalczyk, P.; Gauden, P. A.; Wiśniewski, M.; Terzyk, A. P.; Furmaniak, S.; Burian, A.; Kaneko, K.; Neimark, A. V., Atomic-scale molecular models of oxidized activated carbon fibre nanoregions: Examining the effects of oxygen functionalities on wet formaldehyde adsorption. *Carbon* **2020**, *165*, 67-81.
- 23. Ranganathan, R.; Rokkam, S.; Desai, T.; Keblinski, P., Generation of amorphous carbon models using liquid quench method: A reactive molecular dynamics study. *Carbon* **2017**, *113*, 87-99.
- 24. Shi, Y., A mimetic porous carbon model by quench molecular dynamics simulation. *The Journal of chemical physics* **2008**, *128* (23), 234707.
- 25. Thompson, M. W.; Dyatkin, B.; Wang, H.-W.; Turner, C. H.; Sang, X.; Unocic, R. R.; Iacovella, C. R.; Gogotsi, Y.; Van Duin, A. C.; Cummings, P. T., An atomistic carbide-derived carbon model generated using reaxff-based quenched molecular dynamics. *C* **2017**, *3* (4), 32.
- 26. Palmer, J.; Llobet, A.; Yeon, S.-H.; Fischer, J.; Shi, Y.; Gogotsi, Y.; Gubbins, K., Modeling the structural evolution of carbide-derived carbons using quenched molecular dynamics. *Carbon* **2010**, *48* (4), 1116-1123.
- Wang, Y.; Fan, Z.; Qian, P.; Ala-Nissila, T.; Caro, M. A., Structure and Pore Size Distribution in Nanoporous Carbon. *Chem. Mater.* **2022**.
- de Tomas, C.; Suarez-Martinez, I.; Vallejos-Burgos, F.; Lopez, M. J.; Kaneko, K.; Marks, N. A., Structural prediction of graphitization and porosity in carbide-derived carbons. *Carbon* **2017**, *119*, 1-9.
- de Tomas, C.; Suarez-Martinez, I.; Marks, N. A., Carbide-derived carbons for dense and tunable 3D graphene networks. *Appl. Phys. Lett.* **2018**, *112* (25), 251907.
- 30. Justo, J. F.; Bazant, M. Z.; Kaxiras, E.; Bulatov, V. V.; Yip, S., Interatomic potential for silicon defects and disordered phases. *Physical review B* **1998**, *58* (5), 2539.
- 31. Marks, N. A., Generalizing the environment-dependent interaction potential for carbon. *Physical Review B* **2000**, *63* (3), 035401.
- 32. Thyagarajan, R.; Sholl, D. S., A database of porous rigid amorphous materials. *Chem. Mater.* **2020,** *32* (18), 8020-8033.
- 33. Stukowski, A., Visualization and analysis of atomistic simulation data with OVITO—the Open Visualization Tool. *Modell. Simul. Mater. Sci. Eng.* **2009**, *18* (1), 015012.
- 34. Ravikovitch, P. I.; Vishnyakov, A.; Neimark, A. V., Density functional theories and molecular simulations of adsorption and phase transitions in nanopores. *Physical Review E* **2001**, *64* (1), 011602.
- 35. Cimino, R. T.; Kowalczyk, P.; Ravikovitch, P. I.; Neimark, A. V., Determination of isosteric heat of adsorption by quenched solid density functional theory. *Langmuir* **2017**, *33* (8), 1769-1779.
- 36. Potoff, J. J.; Siepmann, J. I., Vapor–liquid equilibria of mixtures containing alkanes, carbon dioxide, and nitrogen. *AlChE J.* **2001**, *47* (7), 1676-1682.
- 37. Martin, M. G.; Siepmann, J. I., Transferable potentials for phase equilibria. 1. United-atom description of n-alkanes. *J. Phys. Chem. B* **1998**, *102* (14), 2569-2577.
- 38. El Ahmar, E.; Creton, B.; Valtz, A.; Coquelet, C.; Lachet, V.; Richon, D.; Ungerer, P., Thermodynamic study of binary systems containing sulphur dioxide: Measurements and molecular modelling. *Fluid Phase Equilib.* **2011**, *304* (1-2), 21-34.

- 39. Dubbeldam, D.; Calero, S.; Ellis, D. E.; Snurr, R. Q., RASPA: molecular simulation software for adsorption and diffusion in flexible nanoporous materials. *Molecular Simulation* **2016**, *42* (2), 81-101.
- 40. Nicholson, W.; Nicholson, D.; Parsonage, N. G., *Computer simulation and the statistical mechanics of adsorption*. Academic Press: 1982.
- 41. Sarkisov, L.; Bueno-Perez, R.; Sutharson, M.; Fairen-Jimenez, D., Materials Informatics with PoreBlazer v4. 0 and the CSD MOF Database. *Chem. Mater.* **2020**, *32* (23), 9849-9867.
- 42. Connolly, M. L., Solvent-accessible surfaces of proteins and nucleic acids. *Science* **1983**, *221* (4612), 709-713.
- 43. Gelb, L. D.; Gubbins, K., Characterization of porous glasses: Simulation models, adsorption isotherms, and the Brunauer– Emmett– Teller analysis method. *Langmuir* **1998**, *14* (8), 2097-2111.
- 44. Thommes, M.; Kaneko, K.; Neimark, A. V.; Olivier, J. P.; Rodriguez-Reinoso, F.; Rouquerol, J.; Sing, K. S., Physisorption of gases, with special reference to the evaluation of surface area and pore size distribution (IUPAC Technical Report). *Pure Appl. Chem.* **2015**, *87* (9-10), 1051-1069.
- 45. Ravikovitch, P. I.; Vishnyakov, A.; Russo, R.; Neimark, A. V., Unified approach to pore size characterization of microporous carbonaceous materials from N2, Ar, and CO2 adsorption isotherms. *Langmuir* **2000**, *16* (5), 2311-2320.
- 46. VersaWin[™] Gas Sorption Data Reduction Software. Quantachrome Instruments: 2018; Vol. 07169 Rev. C 05/18.
- 47. Babu, D. J.; Puthusseri, D.; Kühl, F. G.; Okeil, S.; Bruns, M.; Hampe, M.; Schneider, J. J., SO2 gas adsorption on carbon nanomaterials: a comparative study. *Beilstein journal of nanotechnology* **2018**, *9* (1), 1782-1792.
- 48. Bläker, C.; Pasel, C.; Luckas, M.; Dreisbach, F.; Bathen, D., Investigation of load-dependent heat of adsorption of alkanes and alkenes on zeolites and activated carbon. *Microporous Mesoporous Mater.* **2017**, *241*, 1-10.
- 49. Bläker, C.; Pasel, C.; Luckas, M.; Dreisbach, F.; Bathen, D., A study on the load-dependent enthalpy of adsorption and interactions in adsorption of C5 and C6 hydrocarbons on zeolites 13X and ZSM-5 and an activated carbon. *Microporous Mesoporous Mater.* **2020**, *302*, 110205.
- 50. Dreisbach, F.; Staudt, R.; Keller, J., High pressure adsorption data of methane, nitrogen, carbon dioxide and their binary and ternary mixtures on activated carbon. *Adsorption* **1999**, *5* (3), 215-227.
- 51. Keller, J. U.; Staudt, R., *Gas adsorption equilibria: experimental methods and adsorptive isotherms*. Springer Science & Business Media: 2005.
- 52. Horváth, G.; Kawazoe, K., Method for the calculation of effective pore size distribution in molecular sieve carbon. *J. Chem. Eng. Jpn.* **1983**, *16* (6), 470-475.

Acknowledgements

The work was supported by the INTERN NSF supplement to the National Science Foundation CBET grant 1834339 and Rutgers undergraduate research Aresty program.

CRediT author statement

Nicholas J. Corrente: Methodology, Validation, Formal Analysis, Investigation, Writing - Original Draft,

Writing – Review & Editing, Visualization

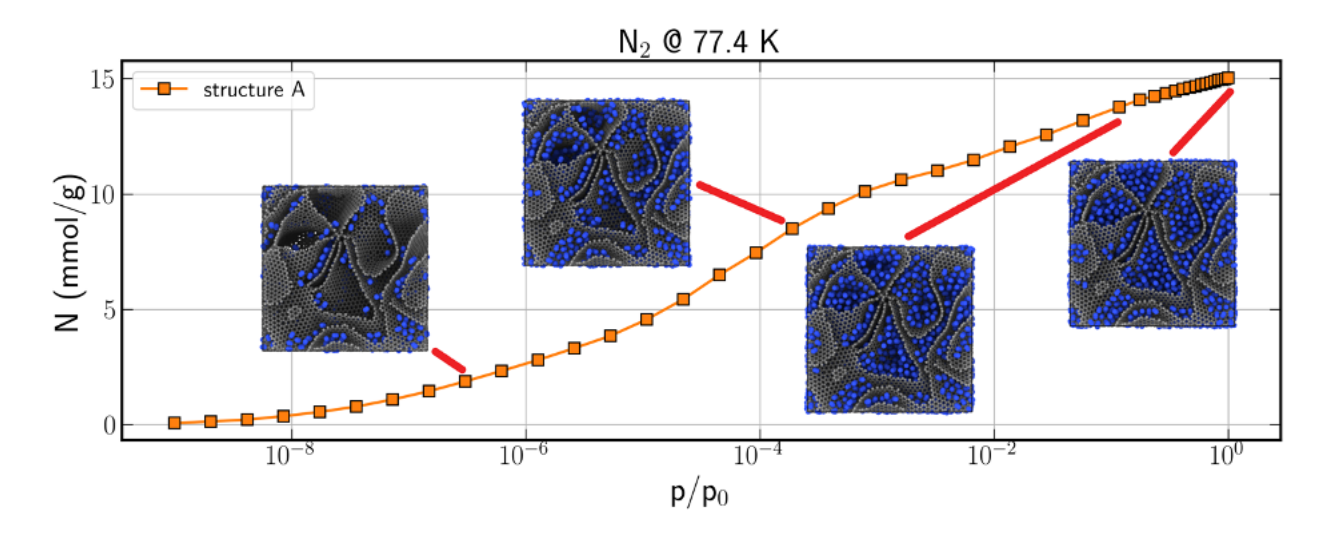
Elizabeth L. Hinks: Investigation, Data curation, Visualization **Aastha Kasera:** Investigation, Data curation, Visualization **Raleigh Gough:** Investigation, Data curation, Visualization

Peter I. Ravikovitch: Methodology, Formal Analysis, Writing – Review & Editing, Supervision

Alexander V. Neimark: Conceptualization, Methodology, Investigation, Writing - Reviewing and Editing,

Supervision

Graphical Abstract:



Highlights:

- Geometric and adsorption methods were used to characterize 3D nanoporous carbon models.
- Molecular simulations with 3D carbon models can be used to predict adsorption of simple fluids and hydrocarbons in activated carbons.